

Supporting Information for

Computational and experimental study of O-glycosylation. Catalysis by human UDP-GalNAc polypeptide:GalNAc transferase-T2.

Hansel Gómez,^{a,b} Raúl Rojas,^c Divya Patel,^c Lawrence A. Tabak,^{*c} José M. Lluch,^{a,b} and Laura Masgrau^{*a}

- ^aInstitut de Biotecnologia i de Biomedicina and ^bDepartament de Química, Universitat Autònoma de Barcelona, 08193 Bellaterra (Cerdanyola del Vallès), Barcelona, Spain.
^c Department of Health and Human Services, Section on Biological Chemistry, National Institute of Dental and Craniofacial Research, National Institutes of Health, Bethesda, MD 20892 (USA)

Experimental Section

Enzyme Assays. The generation of human GalNAc-T2-pIMFK4, a construct used to transfect COS-7 cells to produce secreted wild-type and mutant GalNAc-T2, has been described before by A. G. Holleboom and coworkers.¹ Mutations in positions R362, E334 and N335 were created with the QuikChange II XL Site Directed Mutagenesis Kit (Agilent Technologies, Santa Clara, CA) according to the manufacturer's procedures. GalNAc-T2-pIMFK4 was used as a template.

COS-7 cells were grown to 75% confluency and the wild-type or mutant GalNAc-T2 constructs were transfected with Lipofectamine-2000 (Life Technologies, Carlsbad, CA) as indicated by the manufacturer specifications. The quantification of mutant and wild-type GalNAc-T2 expression levels was performed by SDS-PAGE followed by Western Blotting using a commercial GalNAc-T2 antibody (Sigma-Aldrich, St. Louis, MO). Densitometry was performed with ImageJ 64.

To measure the ability of mutant or wild-type GalNAc-T2 to transfer GalNAc into the EA2 peptide we followed a protocol described before by F. K. Hagen and coworkers.² In short, reactions (25 μ l) containing 500 μ M EA2, 2 mM UDP-GalNAc, 0.4 μ Ci UDP-[1-¹⁴C]GalNAc, 10 mM MnCl₂, 0.1 % Triton-X100, 40 mM 2-mercaptoethanol, 40 mM cacodylate (pH6.5) were mixed with different volumes, but equivalent (as determined by densitometry) amounts, of mutant or wild-type GalNAc-T2 for 1 h at 37°C. Reactions were stopped with 75 μ L of 0.1% trifluoroacetic acid. The EA2 glyco-peptide was purified using Sep-Pak reversed-phase columns. Radioactive GalNAc incorporated into the EA2 peptide was determined by liquid scintillation.

References

- 1 A. G. Holleboom, H Karlsson, R.S. Lin, T. M Beres, J. A. Sierts, D. S. Herman, E. S. G. Stroes, J. M. Aerts, J. J. P. Kastelein, M. M. Motazacker, G. M. Dallinga-Thie, J. H. M. Levels, A. H. Zwinderman, J. G. Seidman, C. E. Seidman, S. Ljunggren, D. J. Lefeber, E. Morava, R. A. Wevers, T. A. Fritz, L. A. Tabak, M. Lindahl, G. K. Hovingh and J. A. Kuivenhoven, *Cell Metabolism*, 2011, **14**, 811.
- 2 F. K. Hagen, K. G. Ten Hagen, T. M. Beres, M. M. Bayls, B. C. VanWuyckhuysen and L. A. Tabak, *J. Biol. Chem.*, 1997, **272**, 13843.

Table S1. QM/MM potential energy barriers and reaction energies (in kcal/mol) for the proposed front-side attack mechanism at different levels of theory in frame 1. The calculations were carried out on the corresponding QM(SCC-DFTB)/MM(CHARMM22) geometries of reactants (R), transition state (TSⁱ) and products (P).

	SCC-DFTB	BP86		B3LYP		M05-2X	
		SVP	TZVP	SVP	TZVP	SVP	TZVP
R	0.0	0.0	0.0	0.0	0.0	0.0	0.0
TSⁱ	39.0	18.8	14.23	22.2	17.4	28.7	22.7
P	13.2	16.5	13.1	15.1	11.6	16.78	13.3

Table S2. Selected QM/MM bond distances d (Å), dihedral angle (Degrees) and atomic charges q (a.u.) in the optimized reactants (R), transition state (TSⁱ), and products (P) for the front-side attack mechanism in frame 1. QM=SCC-DFTB and M05-2X/TZVP//BP86/SVP for the distances and charges respectively.

	Reactants	TS ⁱ	Products
$d(\text{O3B}_{\text{UDP}}-\text{C1}'_{\alpha\text{-GalNAc}})$	1.48	2.59	3.20
$d(\text{OG1}_{\text{T7}}-\text{C1}'_{\alpha\text{-GalNAc}})$	2.82	2.40	1.49
$d(\text{HG1}_{\text{T7}}-\text{OG1}_{\text{T7}})$	0.99	1.24	2.55
$d(\text{HG1}_{\text{T7}}-\text{O3B}_{\text{UDP}})$	1.85	1.17	0.98
$d(\text{O}_{\text{A307}}-\text{C1}'_{\alpha\text{-GalNAc}})$	4.14	3.14	3.24
$d(\text{C1}'_{\alpha\text{-GalNAc}}-\text{O5}'_{\alpha\text{-GalNAc}})$	1.45	1.28	1.45
$d(\text{HN2}'_{\alpha\text{-GalNAc}}-\text{O1B}_{\text{UDP}})$	2.03	1.75	1.85
$(\text{H2}'-\text{C2}'-\text{N2}'-\text{HN2}')_{\alpha\text{-GalNAc}}$	167.19	164.19	152.28
$q(\text{C1}'_{\alpha\text{-GalNAc}})$	0.37	0.59	0.37
$q(\text{O3B}_{\text{UDP}})$	-0.87	-1.12	-0.99
$q(\text{O5}'_{\alpha\text{-GalNAc}})$	-0.52	-0.40	-0.54
$q(\text{O1B}_{\text{UDP}})$	-1.16	-1.20	-1.16
$q(\text{HN2}'_{\alpha\text{-GalNAc}})$	0.48	0.49	0.46

As we had seen in our study of LgtC and α 3GalT, the QM(SCC-DFTB)MM (CHARMM22) level of theory tends to give sharper potential energy profiles and considerably overestimates the potential energy values (energy barrier of 38.95 kcal/mol), although single point calculations at the reference method (QM = M05-2X/TZVP) yielded an energy barrier of 22.72 kcal/mol. The transition state also tends to be less dissociative (TSⁱ $d(\text{O3B}_{\text{UDP}}-\text{C1}'_{\alpha\text{-GalNAc}}) = 2.59$ Å) than the QM = BP86/SVP result (?TSⁱ $d(\text{O3B}_{\text{UDP}}-\text{C1}'_{\alpha\text{-GalNAc}}) = 3.10$ Å)).

Table S3. QM/MM potential energy barriers and reaction energies (in kcal/mol) for the proposed front-side attack mechanism at different levels of theory in frame 2. The calculations were carried out on the corresponding QM(BP86/SVP)/MM(CHARMM22) geometries of reactants (R), transition state guess (?TSⁱ) and products (P).

	BP86		B3LYP		M05-2X	
	SVP	TZVP	SVP	TZVP	SVP	TZVP
R	0.0	0.0	0.0	0.0	0.0	0.0
?TSⁱ	15.67	10.7	19.3	13.89	26.8	20.2
P	1.5	-0.9	0.9	-1.6	2.8	-0.1

Table S4. Selected QM/MM bond distances d (Å), dihedral angle (Degrees) and atomic charges q (a.u.) in the optimized reactants (R), transition state guess (?TSⁱ), and products (P) for the front-side attack mechanism in frame 1. QM=BP86/SVP and M05-2X/TZVP//BP86/SVP for the geometrical parameters and charges, respectively.

	Reactants	?TS ⁱ	Products
$d(\text{O3B}_{\text{UDP}}-\text{C1}'_{\alpha\text{-GalNAc}})$	1.51	3.10	3.30
$d(\text{OG1}_{\text{T7}}-\text{C1}'_{\alpha\text{-GalNAc}})$	2.86	2.20	1.49
$d(\text{HG1}_{\text{T7}}-\text{OG1}_{\text{T7}})$	0.99	1.15	1.47
$d(\text{HG1}_{\text{T7}}-\text{O3B}_{\text{UDP}})$	1.79	1.24	1.02
$d(\text{O}_{\text{A307}}-\text{C1}'_{\alpha\text{-GalNAc}})$	4.09	3.12	3.25
$d(\text{C1}'_{\alpha\text{-GalNAc}}-\text{O5}'_{\alpha\text{-GalNAc}})$	1.38	1.29	1.39
$d(\text{HN2}'_{\alpha\text{-GalNAc}}-\text{O1B}_{\text{UDP}})$	2.31	1.91	2.09
$(\text{H2}'-\text{C2}'-\text{N2}'-\text{HN2}')_{\alpha\text{-GalNAc}}$	164.5	168.0	158.8
$q(\text{C1}'_{\alpha\text{-GalNAc}})$	0.39	0.57	0.37
$q(\text{O3B}_{\text{UDP}})$	-0.91	-1.16	-1.07
$q(\text{O5}'_{\alpha\text{-GalNAc}})$	-0.51	-0.44	-0.56
$q(\text{O1B}_{\text{UDP}})$	-1.18	-1.23	-1.20
$q(\text{HN2}'_{\alpha\text{-GalNAc}})$	0.47	0.49	0.46

Table S5. Selected QM/MM bond distances d (Å), dihedral angle (Degrees) and atomic charges q (a.u.) in the optimized reactants (R), transition state guess (?TSⁱ), and products (P) for the front-side attack mechanism in frame 2. QM=BP86/SVP and M05-2X/TZVP//BP86/SVP for the geometrical parameters and charges, respectively.

	Reactants	?TS ⁱ	Products
$d(\text{O3B}_{\text{UDP}}-\text{C1}'_{\alpha\text{-GalNAc}})$	1.51	3.13	3.36
$d(\text{OG1}_{\text{T7}}-\text{C1}'_{\alpha\text{-GalNAc}})$	2.86	2.24	1.49
$d(\text{HG1}_{\text{T7}}-\text{OG1}_{\text{T7}})$	0.99	1.16	1.48
$d(\text{HG1}_{\text{T7}}-\text{O3B}_{\text{UDP}})$	1.79	1.23	1.02
$d(\text{O}_{\text{A307}}-\text{C1}'_{\alpha\text{-GalNAc}})$	4.11	3.10	3.25
$d(\text{C1}'_{\alpha\text{-GalNAc}}-\text{O5}'_{\alpha\text{-GalNAc}})$	1.38	1.29	1.39
$d(\text{HN2}'_{\alpha\text{-GalNAc}}-\text{O1B}_{\text{UDP}})$	2.32	1.90	2.04
$(\text{H2}'-\text{C2}'-\text{N2}'-\text{HN2}')_{\alpha\text{-GalNAc}}$	163.73	167.53	158.68
$q(\text{C1}'_{\alpha\text{-GalNAc}})$	0.40	0.57	0.37
$q(\text{O3B}_{\text{UDP}})$	-0.91	-1.16	-1.07
$q(\text{O5}'_{\alpha\text{-GalNAc}})$	-0.51	-0.43	-0.56
$q(\text{O1B}_{\text{UDP}})$	-1.18	-1.23	-1.20
$q(\text{HN2}'_{\alpha\text{-GalNAc}})$	0.47	0.49	0.47

Table S6. Donor-Acceptor Natural Bond Orbitals (NBO) analysis for the front-side attack mechanism in wild-type ppGaNAcT-2 for frame 1. QM=(M05-2X/TZVP//BP86/SVP). LP: lone pair; BD: bonding molecular orbital; BD*: antibonding molecular orbital; CR: core pair. Only the main interacting pairs are given. ΔE corresponds to the energy difference between the interacting molecular orbitals in the transition state guess (?TSⁱ) and the reactants (R). [&], [§] Interactions only present in R or ?TSⁱ, respectively. Reference to the Figure where the interaction is depicted is given within parenthesis.

Donor NBO	Acceptor NBO	ΔE (kcal/mol)
UDP-GalNAc – Thr 7 (EA2)		
BD ₂ (PB-O3B) _{UDP}	BD* ₁ (OG1-HG1) _{T7}	125.0 [§] (4B)
LP ₂ (OG1) _{T7}	BD* ₂ (C1'-O5') _{α-GalNAc}	25.7
BD* ₁ (PB-O3B) _{UDP}	BD* ₁ (OG1-HG1) _{T7}	14.1 [§]
LP ₁ (O3B) _{UDP}	BD* ₁ (OG1-HG1) _{T7}	12.2
BD ₁ (PB-O3B) _{UDP}	BD* ₁ (OG1-HG1) _{T7}	5.0 [§]
CR ₁ (O3B) _{UDP}	BD* ₁ (OG1-HG1) _{T7}	3.8 [§]
BD* ₁ (OG1-HG1) _{T7}	BD* ₂ (PB-O3B) _{UDP}	3.6 [§]
BD ₁ (OG1-HG1) _{T7}	BD* ₂ (C1'-O5') _{α-GalNAc}	3.2
LP ₁ (OG1) _{T7}	BD* ₂ (C1'-O5') _{α-GalNAc}	2.4
LP ₃ (O3B) _{UDP}	BD* ₁ (N-HN) _{T7}	2.1 (4D)
LP ₂ (O3B) _{UDP}	BD* ₁ (N-HN) _{T7}	1.4
BD* ₁ (OG1-HG1) _{T7}	BD* ₁ (C1'-H1') _{α-GalNAc}	1.0
LP ₁ (O3B) _{UDP}	BD* ₁ (N-HN) _{T7}	-2.01 (4C)
LP ₂ (O3B) _{UDP}	BD* ₁ (OG1-HG1) _{T7}	-8.7 (4A)
NAc – Asp224/UDP		
LP ₁ (O1B) _{UDP}	BD* ₁ (N2'-HN2') _{α-GalNAc}	6.9 [§] (4F)
BD* ₁ (PB-O1B) _{UDP}	BD* ₁ (N2'-HN2') _{α-GalNAc}	2.5 [§]
LP ₂ (O1B) _{UDP}	BD* ₁ (N2'-HN2') _{α-GalNAc}	2.1 [§]
LP ₃ (O1B) _{UDP}	BD* ₁ (N2'-HN2') _{α-GalNAc}	1.2 [§]
LP ₃ (OD2) _{D224}	BD* ₁ (N2'-HN2') _{α-GalNAc}	-2.1 ^{&}
LP ₁ (OD2) _{D224}	BD* ₁ (N2'-HN2') _{α-GalNAc}	-7.3 ^{&} (4E)

Table S7. Quantification and normalization of secreted recombinant wild type and mutant GalNAc-T2. See Figure S8 for a representative Western blot run and later used for protein quantification.

Enzyme	Secreted hT2 (A.U)	Background (A.U)	SecretedT2- background (A.U)	Normalize ratio to WT	Vol. (μl) of COS-7 cell supernatant/ reaction
WT	72	11	61	1	5
E334Q	102	14	88	~1.5	3.3
N335A	117	15	102	~1.7	2.9
N335D	129	16	113	~1.9	2.6
N335H	84	14	70	~1.2	4.2
N335S	111	20	91	~1.5	3.3
R362K	135	18	117	~1.9	2.6

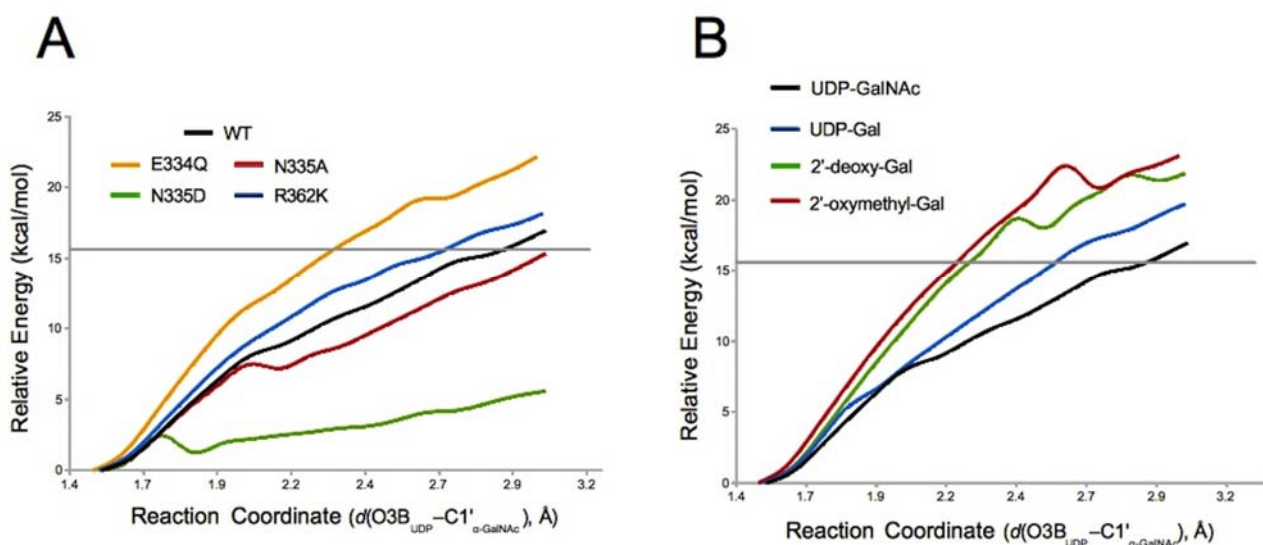


Figure S1. QM(BP86/SVP)/MM(CHARMM22) energy profiles for the UDP-GalNAc bond-breaking process in (A) GalNAc-T2 mutants with the UDP-GalNAc donor and in (B) wild-type GalNAc-T2 with different donor substrates. The horizontal grey line indicates the energy barrier estimated at this level of calculation for the front-side attack mechanism for the WT enzyme with UDP-GalNAc as the donor substrate.

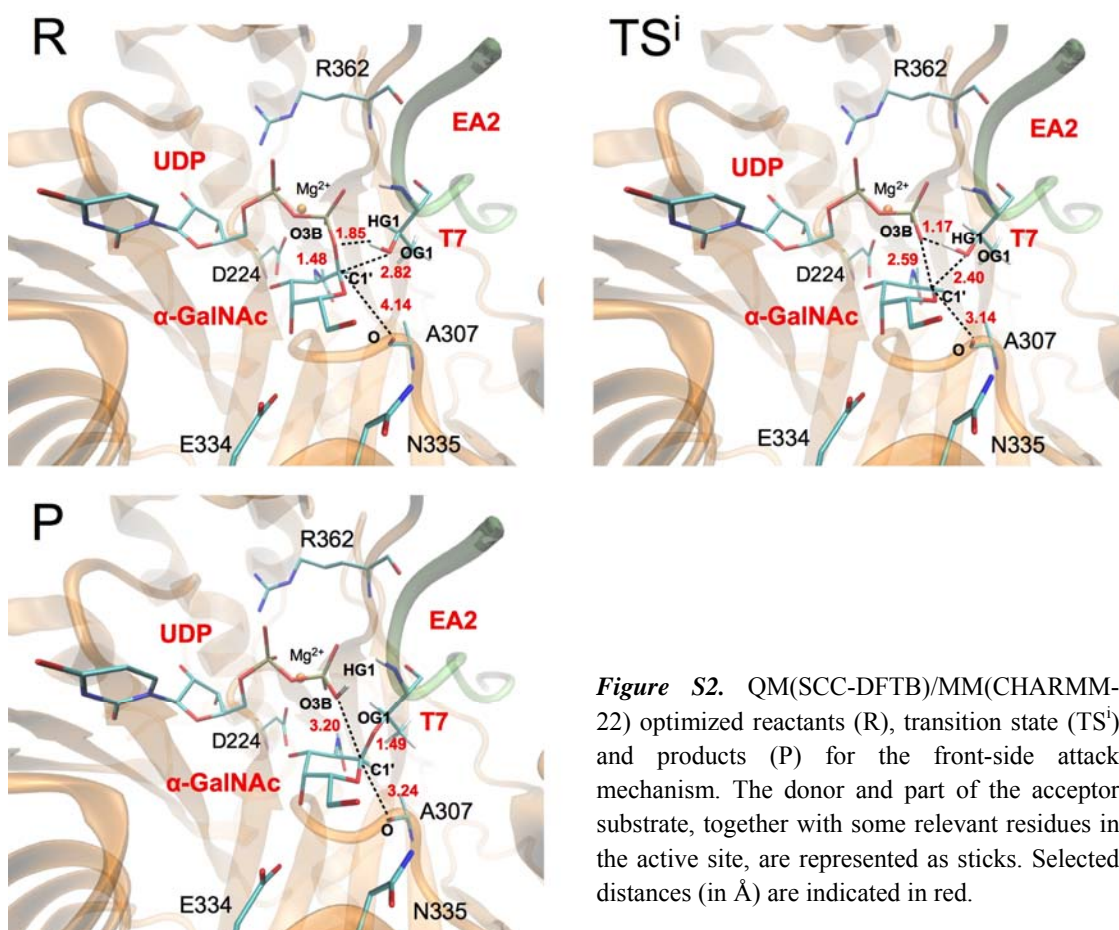


Figure S2. QM(SCC-DFTB)/MM(CHARMM-22) optimized reactants (R), transition state (TSⁱ) and products (P) for the front-side attack mechanism. The donor and part of the acceptor substrate, together with some relevant residues in the active site, are represented as sticks. Selected distances (in Å) are indicated in red.

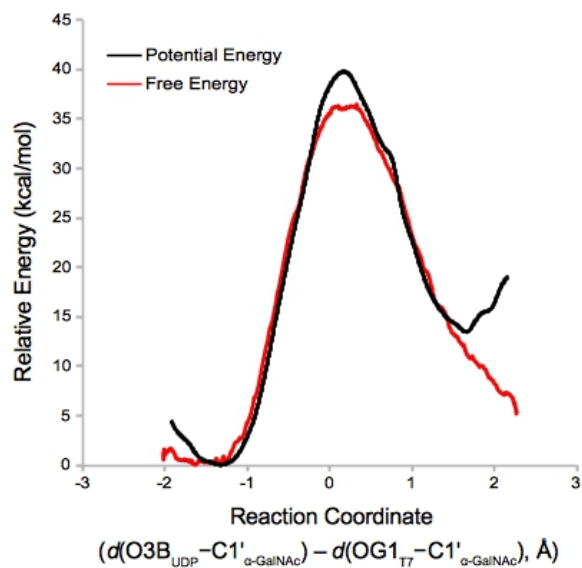


Figure S3. SCC-DFTB/CHARMM22 potential energy profile and potential of mean force (PMF) for the front-side attack mechanism in frame 1. Umbrella sampling at the SCC-DFTB/CHARMM22 level was performed to compute the potential of mean force (PMF) and the free energy profile for the front-side attack mechanism using the dynamics module within ChemShell. The reaction coordinate defined as $RC = [d(O3B_{UDP}-C1'_{\alpha-GalNAc}) - d(OG1_{T7}-C1'_{\alpha-GalNAc})]$ was scanned in steps of 0.1 Å, with a force constant of $237 \text{ kcal mol}^{-1} \text{ \AA}^{-2}$ and with 5 ps of data collection for every sampling window. The weighted histogram analysis method (WHAM)[S. Kumar et al., *J. Comput. Chem.*, 1992, **13**, 1011; M. Souaille, *Comput. Phys. Commun.*, 2001, **135**, 40] was used to compute the free energy profile.

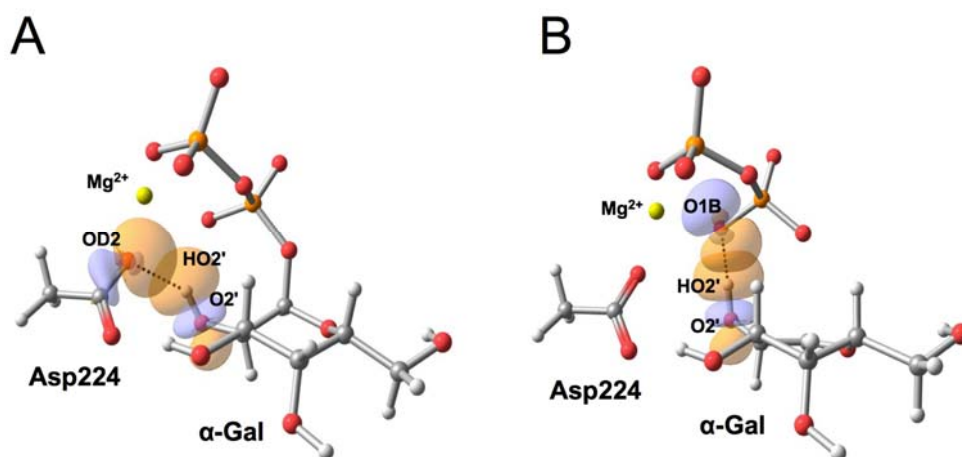


Figure S4. Interactions between molecular orbitals of the 2' hydroxyl group of Gal with (A) Asp224 and (B) UDP in R and $?TS^{\ddagger}$, respectively, and according to a NBO analysis in ppGaNAcT-2. For clarity, just a fraction of the QM atoms is shown.

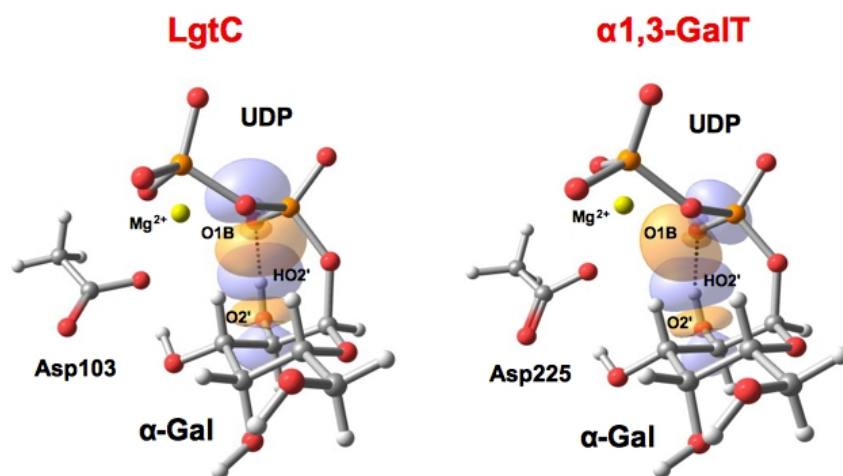


Figure S5. Interactions between molecular orbitals of the 2'-hydroxyl group of Gal and UDP in the LgtC and α 1,3-GalT Michaelis complexes (R) according to a NBO analysis. The interactions are only depicted in the reactants. For clarity, just a fraction of the QM atoms is shown.

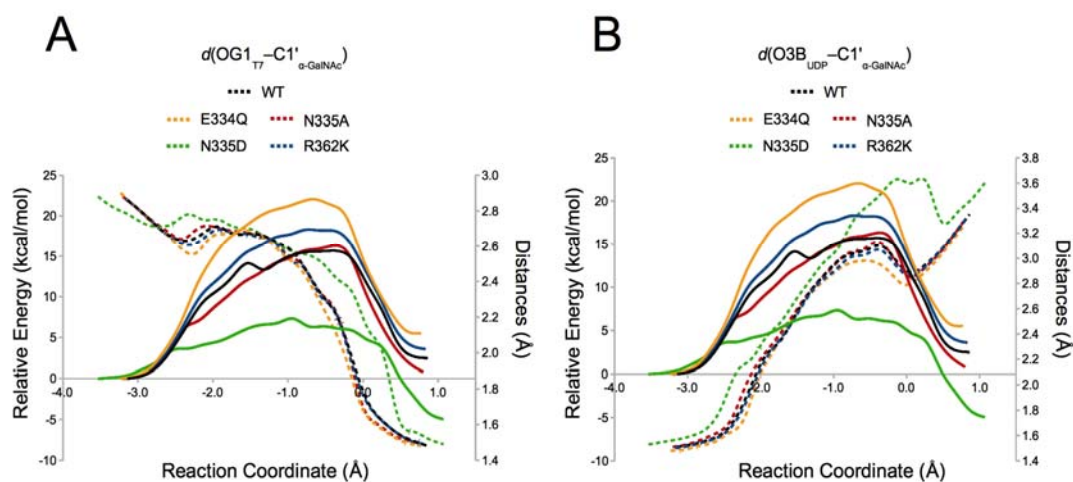
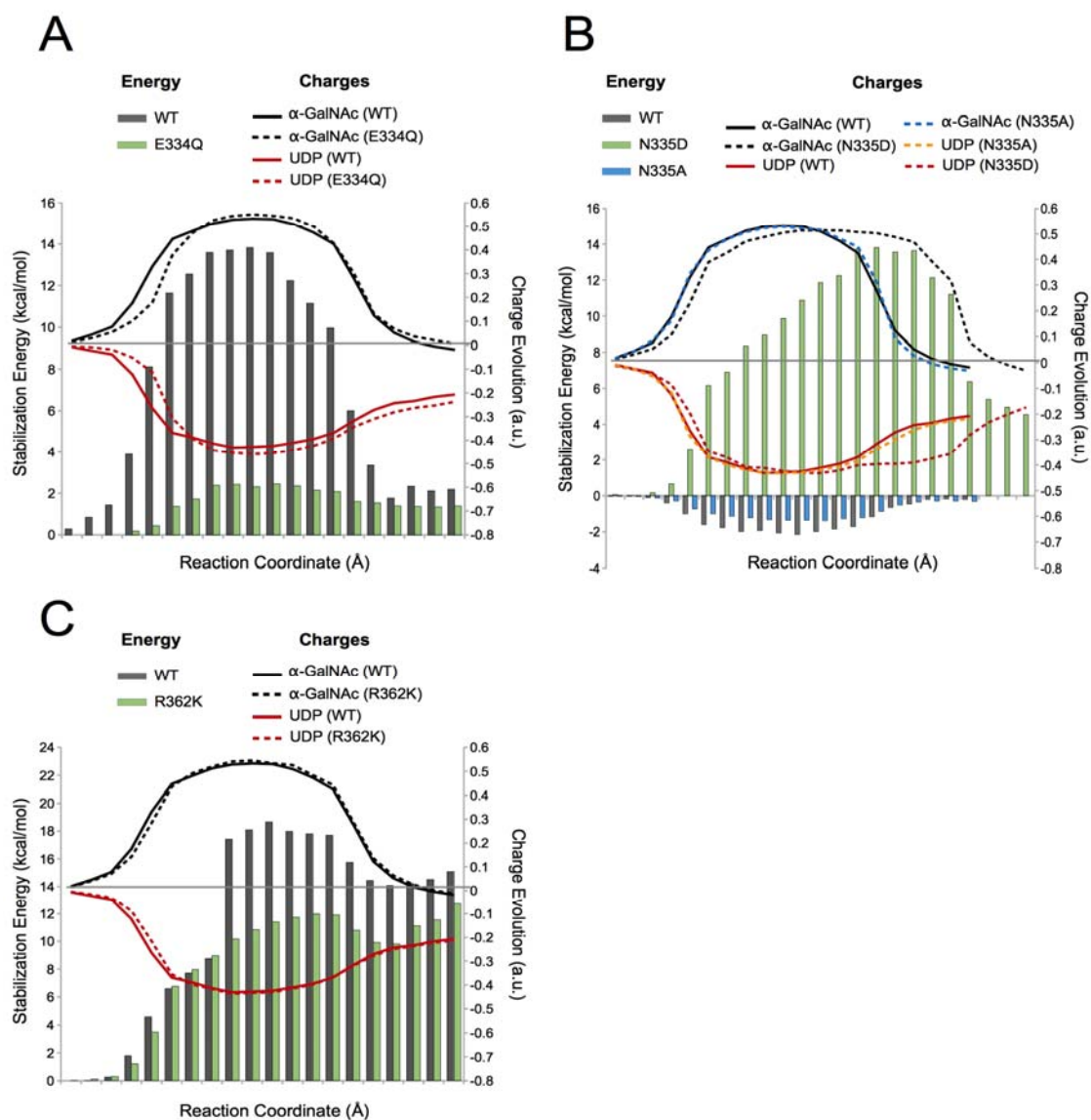


Figure S6. QM(BP86/SVP)/MM(CHARMM22) energy profile for the front-side attack mechanism in wild-type (WT) ppGalNAcT-2 and mutants E334Q, N335A, N335D and R362K. Reaction coordinate (RC) = $[d(O3B_{UDP}-C1'_{\alpha-GalNAc}) - d(OG1_{T7}-C1'_{\alpha-GalNAc}) - d(HG1_{T7}-O3B_{UDP})]$. The variation of (A) $d(OG1_{T7}-C1'_{\alpha-GalNAc})$ and (B) $d(O3B_{UDP}-C1'_{\alpha-GalNAc})$ is also shown. Solid lines correspond to the QM/MM potential energy profiles and follow the same color code used for the distances.

S7.



Figure

Electrostatic contribution to the stabilization of the QM region along the front-side attack mechanism by residues in position 334 (A), 335 (B) and 362 (C). In each case the wild-type (WT) enzyme and the corresponding mutant/s were considered. QM = M05-2X/TZVP. The charge evolution of the α -GalNAc ring and UDP is also given. Reaction Coordinate (RC) = $[d(O3B_{UDP}-C1'_{\alpha-GalNAc})-d(OG1_{T7}-C1'_{\alpha-GalNAc})-d(HG1_{T7}-O3B_{UDP})]$.

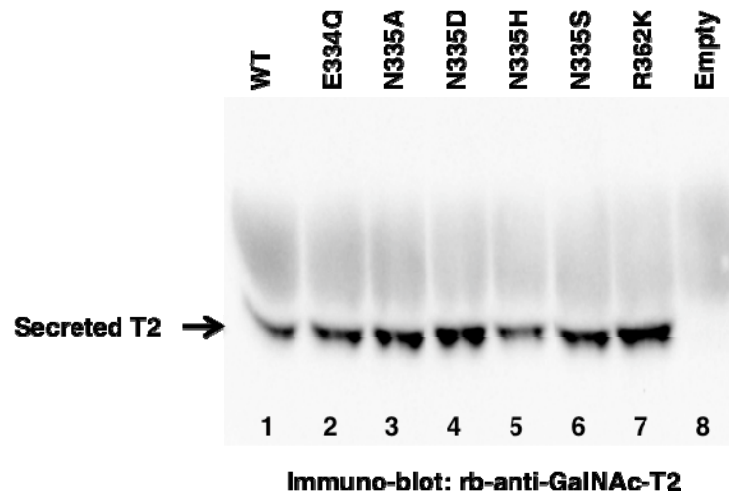


Figure S8. COS-7 cells were transfected with plasmids encoding wild-type (lane 1) or mutant GalNAc-T2 (lane 2 through 7), or the empty pIMFK4 plasmid (lane 8). After 96 h, cell media containing secreted wild-type or mutant GalNAc-T2 was collected and later analyzed by SDS-PAGE and immunoblotting with a rabbit polyclonal antibody to GalNAc-T2. Table S7 shows the results of the quantification done by densitometry of the different levels of expression of each mutant relative to wild-type GalNAc-T2. The adjusted volumes of COS-7 cell media used in the enzymatic assays are also shown.